

NOBLE GAS INVENTORY OF MICROMETEORITES FROM THE TRANSANTARCTIC MOUNTAINS.

B. Baecker^{1,4}, C. Cordier², L. Folco³, M. Trierloff⁴, J. A. Cartwright¹ and U. Ott¹, ¹Abteilung Biogeochemie, Max-Planck-Institut für Chemie, Joh.-Joachim-Becher-Weg 27, 55128 Mainz, Germany. E-mail: b.baecker@mpic.de
²ISTerre, Université de Grenoble, CNRS, F-38041 Grenoble, France. ³Dipartimento di Scienze della Terra, Università di Pisa, Via S.Maria 53,56126 Pisa, Italy. ⁴Institut für Geowissenschaften, Universität Heidelberg, Im Neuenheimer Feld 236, 69120 Heidelberg, Germany.

Introduction: We have initiated a comprehensive survey of noble gases in micrometeorites (MMs) at the MPIC, Mainz. While the lighter noble gases (especially neon) are generally dominated by solar wind contributions, the inventory of the heavy primordial noble gases is not well characterized. We hope to fill this gap, with a focus on the diagnostic isotopic composition of xenon. Here, we present initial results obtained on “large” MMs from Victoria Land, Transantarctic Mountains. These were collected during a PNRA (Programma Nazionale delle Ricerche in Antartide, Italy) expedition on top of the Miller Butte micrometeorite traps #45 b and c [1]. Our future noble gas research will include material from other collections, e.g. CONCORDIA [2].

Samples: We selected 51 samples for our study: 26 cosmic spherules (CS), 11 scoriaceous (Sc) and 14 unmelted (Un), in the ~600-800 µm size range (Fig. 1). They were split into aliquots, of which one remained in Siena for SEM and microprobe analyses and the other was taken to the MPIC Mainz for noble gas analysis.

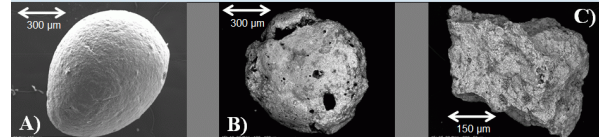


Fig. 1: Micrographs of MMs from the Transantarctic mountains. A) cosmic spherule, B) scoriaceous and C) unmelted.

Analytical procedures: Noble gases were released using laser heating (CO₂ laser), cleaned with SAES getters and separated into He/Ne, Ar, Kr and Xe fractions using activated charcoal. The analyses were performed using our high sensitivity Noblesse (Nu Instruments) noble gas mass spectrometer with multi-ion-detection (8 channeltrons) [3].

Results and Discussion: At present, we have obtained noble gas results for three CS, four Sc and four Un MMs. Our results are summarized in Table 1 and

Figures 2-4.

Neon: Noble gas abundances in CS are low, and Ne isotopic compositions are indistinguishable from air (Fig. 2). Solar wind (SW)-type and spallogenic contributions are evident in Sc and Un MMs, however, with the latter particularly prominent in Sc 45b08 (Fig. 2). The highest concentration of cosmogenic ²¹Ne of ~0.86 x 10⁻⁸ cc/g found in this sample (Table 1) corresponds to a cosmic ray exposure (CRE) age of ~0.75 Ma, if the combined GCR + SCR production rate for very small particles at 1 AU from [4] is used. The highest measured concentration of trapped (solar) ²⁰Ne of ~3.46 x 10⁻⁶ cc/g in Un X1 is in the lower range of those observed in MMs from Dome Fuji [4], but clearly higher than in CS (Table 1; Table 4 in [13]).

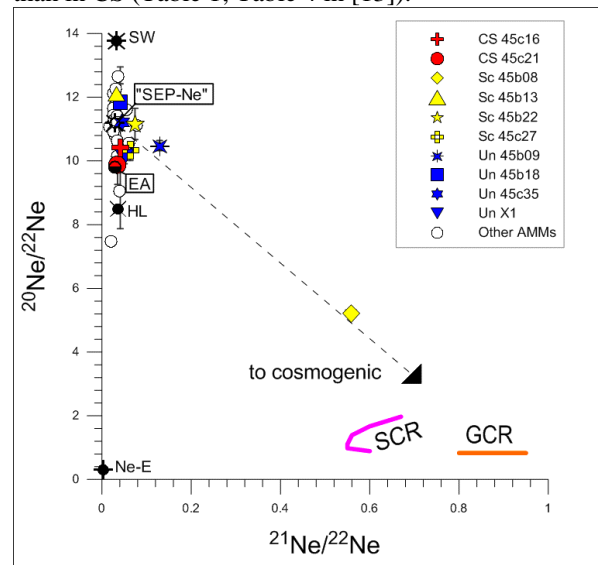


Fig. 2. Three isotope plot of ²⁰Ne/²²Ne vs. ²¹Ne/²²Ne for our data and data from [4]. Also plotted for comparison are SW [5], SEP-Ne [6], Earth atmosphere (EA) [7], HL [8], Ne-E[9], GCR [10] and the compositions of SCR - calculated from Mg, Al, Si at 0.50-10.0 g/cm² [11] using CM chondrite composition [12].

Table 1. Ne, Ar, Kr and Xe results for CS, Sc and Un MMs. Noble gas amounts (*) in 10⁻¹² cc units, concentrations (#) in 10⁻⁸ cc/g. CRE-ages are calculated using the combined GCR+SCR production rates at 1AU from [4]. Uncertainties are given in parentheses. Corrected for blank.

Samples	Size [µm]	Weight [µg]	²² Ne (*)	²⁰ Ne/ ²² Ne	²¹ Ne/ ²² Ne	²¹ Ne _{cos} (#)	²⁰ Ne _{trap} (#)	CRE ages (Ma)	⁴⁰ Ar/ ³⁶ Ar	³⁶ Ar/ ¹³² Xe	⁸⁴ Kr/ ¹³² Xe	¹³² Xe (*)
CS45c16	465x324	105.1 (1)	0.10 (4)	10.4 (2.5)	0.041 (10)	n.a.	1.0 (5)	n.a.	345 (63)	n.a.	n.a.	n.a.
CS45c21	720x556	337.9 (2)	0.31 (3)	9.88 (62)	0.035 (4)	n.a.	0.9 (1)	n.a.	n.a.	n.a.	n.a.	n.a.
Sc45b08	654x374	119.3 (1)	1.88 (4)	5.23 (7)	0.558 (12)	0.858 (26)	7.4 (5)	0.746 (23)	260 (6)	44 (3)	5.4 (6)	0.080 (4)
Sc45b13	547x455	137.6 (1)	3.45 (6)	12.12 (19)	0.033 (1)	0.007 (6)	30 (2)	0.006 (5)	217 (5)	62 (5)	3.6 (3)	0.405 (31)
Sc45b22	268x191	9.2 (1)	0.40 (3)	11.16 (49)	0.074 (5)	0.194 (24)	49 (5)	0.169 (21)	45 (35)	n.a.	n.a.	n.a.
Sc45c27	521x337	38.0 (1)	0.62 (4)	10.35 (34)	0.063 (5)	0.019 (3)	6.4 (6)	0.017 (3)	225 (7)	77 (48)	4.0 (2.4)	0.0078 (47)
Un45b09	626x557	126.9 (1)	7.95 (13)	10.48 (16)	0.129 (2)	0.644 (18)	65 (4)	0.560 (16)	66 (3)	59 (5)	2.3 (2)	0.103 (8)
Un45b18	253x235	5.3 (1)	0.36 (3)	11.86 (56)	0.041 (4)	0.074 (25)	81 (9)	0.064 (22)	193 (8)	n.a.	n.a.	n.a.
Un45c35	428x245	29.0 (1)	3.00 (9)	11.22 (26)	0.044 (1)	0.164 (26)	116 (8)	0.143 (23)	2.27 (75)	143 (6)	0.6 (1)	0.305 (11)
UnX1	427x315	35.0 (1)	12.00 (17)	10.12 (21)	0.050 (1)	0.730 (75)	346 (21)	0.635 (65)	54 (1)	1718 (175)	3.8 (9)	0.010 (1)

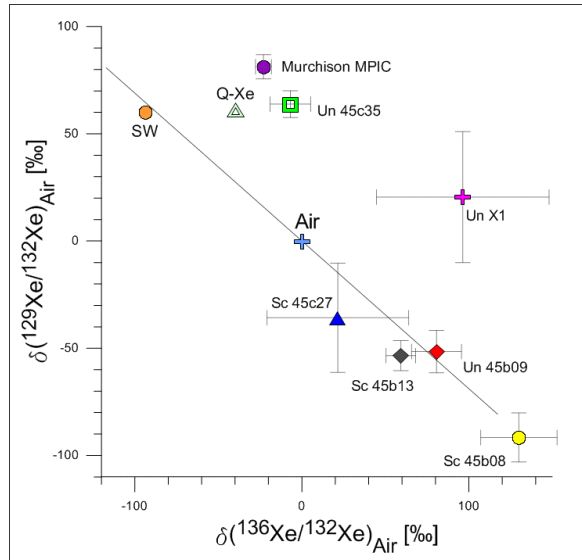


Fig. 3. Three isotope plot of $^{129}\text{Xe}/^{132}\text{Xe}$ vs. $^{136}\text{Xe}/^{132}\text{Xe}$ showing our data compared to Murchison (measured at MPIC 2011), SW [17] and Q-Xe [14] and Q-Xe [15]. Isotope ratios shown in per mil-deviations from air Xe [16] composition.

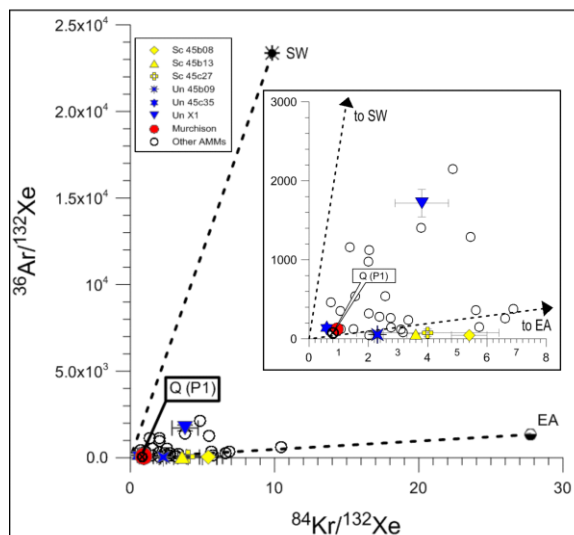


Fig. 4. Elemental ratio plot of $^{36}\text{Ar}/^{132}\text{Xe}$ vs. $^{84}\text{Kr}/^{132}\text{Xe}$ for our data and data from [4], featuring also SW [17], EA [18] and Q (P1) [15].

Argon, krypton and xenon: As evident from the low $^{40}\text{Ar}/^{36}\text{Ar}$ ratios in most of our MMs (Table 1), the primordial Ar isotopes are dominated by an extraterrestrial component, with air contamination making a smaller contribution. While previous research [1, 19] suggested that large MMs show relationship to ordinary rather than carbonaceous chondrite composition, the low $^{40}\text{Ar}/^{36}\text{Ar}$ ratios are not consistent with ordinary chondrites, where $^{40}\text{Ar}/^{36}\text{Ar}$ ratios are typically much higher than in air (see [20]). The lowest ratio (2.27 ± 0.75) is observed in the unmelted MM 45c35 (Table 1), which also contains Xe with an isotopic composi-

tion close to the “planetary” P1 (Q) component [15], and this is typically found in bulk CM chondrites like Murchison (Fig. 3). Note that this is the first precise Xe analysis in MMs, and it indicates a relation to meteorites of the CM/CI type. In the elemental ratio plot $^{36}\text{Ar}/^{132}\text{Xe}$ vs. $^{84}\text{Kr}/^{132}\text{Xe}$ (Fig. 4), 45c35 plots in the carbonaceous chondrite region. In contrast, the other samples (except SW-rich MM Un X1) are characterized by low $^{36}\text{Ar}/^{132}\text{Xe}$ and high $^{84}\text{Kr}/^{132}\text{Xe}$ (compared to meteorites), which is typical for contamination by fractionated air, e.g. [21]; [22]. Air contamination of the samples is also highlighted by Fig. 3, where these MMs show a composition consistent with fractionated air (though, fractionated SW cannot be ruled out based on the isotopic data alone). In general, air contamination from adsorption or attributed to weathering is not accompanied by noticeable isotopic fractionation (e.g. [18]; [23]), and to our knowledge, experimental work leading to isotopic effects has always included ionized noble gases ([24]; [25]). Further work is needed to ascertain the origin of the apparently mass fractionated Xe observed here to determine whether it was acquired during residence on Earth or during passage through the atmosphere.

References: [1] Rochette P. et al. (2008) *PNAS*, 105, 18206-18211. [2] Duprat J. et al. (2007) *Adv. Space Res.*, 39, 605-611. [3] Ott U. et al. (2010) *73rd Ann. Met. Soc. Meeting* (Abs. #5096). [4] Osawa T. and Nagao K. (2002) *MAPS*, 37, 911-936. [5] Heber et al. (2009) *GCA*, 73, 7414-7432. [6] Benkert J.-P. et al. (1993) *J. Geophys. Res.*, 98, 13147-13162. [7] Eberhardt P. et al. (1965) *Z. Naturforschung*, 20a, 623-624. [8] Huss G. R. and Lewis R. S. (1994) *Meteoritics*, 29, 811-829. [9] Lewis et al. (1994) *GCA*, 58, 471-494. [10] Garrison et al. (1995) *Meteoritics*, 30, 738-747. [11] Reedy R. C. (1992) *LPS XXIII* (Abs. #1133). [12] Wasson J. T. and Kallemeyn G. W. (1988) *Phil. Trans. R. Soc. Lond.*, A325, 535-544. [13] Osawa T. et al. (2010) *MAPS*, 45, 1320-1339. [14] Pepin R.O. et al. (1995) *GCA*, 59, 4997-5022. [15] Busemann H. et al. (2000) *MAPS*, 35, 949-973. [16] Basford, J.R. et al. (1973) *Proc. 4th Lunar Sci. Conf.*, *GCA Suppl.* 4, 1915-1955. [17] Vogel et al. (2011) *GCA*, 75, 3057-3071. [18] Ozima M. and Podosek F.A. (2001) *Noble Gas Geochemistry*, Cambridge Univ. Press. [19] Dobrică et al. (2011) *MAPS*, 46, 1363-1375. [20] Schultz L. and Franke L. (2004) *MAPS*, 39, 1889-1890. [21] Scherer P. et al. (1994) *Noble Gas Geochemistry and Cosmochemistry*, 43-53, TERRAPUB, Tokyo. [22] Schwenzer S. P. (2007) *LPS XXXVIII* (Abs. #1150). [23] Podosek F. A. et al. (1981) *GCA*, 45, 2401-2415. [24] Nichols Jr. R. H. et al. (1992) *Meteoritics*, 27, 555-559. [25] Hohenberg C.M. et al. (2002) *MAPS*, 37, 257-267.